STEM CELLS®

EMBRYONIC STEM CELLS/INDUCED PLURIPOTENT STEM CELLS

SMAD7 Directly Converts Human Embryonic Stem Cells to Telencephalic Fate by a Default Mechanism

MOHAMMAD ZEESHAN OZAIR, SCOTT NOGGLE, ARYEH WARMFLASH, JOANNA ELA KRZYSPIAK, ALI H. BRIVANLOU

Laboratory of Molecular Embryology, The Rockefeller University, New York, New York, USA

Key Words. Human embryonic stem cells • Neural induction • Neural differentiation • TGFβ • MEK

ABSTRACT

Human embryonic stem cells (hESCs) provide a valuable window into the dissection of the molecular circuitry underlying the early formation of the human forebrain. However, dissection of signaling events in forebrain development using current protocols is complicated by non-neural contamination and fluctuation of extrinsic influences. Here, we show that SMAD7, a cell-intrinsic inhibitor of transforming growth factor-β (TGFβ) signaling, is sufficient to directly convert pluripotent hESCs to an anterior neural fate. Time course gene expression revealed downregulation of MAPK components, and combining MEK1/2 inhibition with SMAD7-mediated TGFβ inhibition promoted telencephalic conversion. Fibroblast growth factor-MEK and TGFβ-SMAD signaling maintain hESCs by promoting pluripotency genes and repressing neural genes. Our findings suggest that in the absence of these cues, pluripotent cells simply revert to a program of neural conversion. Hence, the "primed" state of hESCs requires inhibition of the "default" state of neural fate acquisition. This has parallels in amphibians, suggesting an evolutionarily conserved mechanism. STEM CELLS *2013;31:35–47*

Disclosure of potential conflicts of interest is found at the end of this article.

INTRODUCTION

The establishment of the embryo's initial lineage that will ultimately give rise to the adult central nervous system (CNS)—a process called neural induction [1]—is a fundamental milestone during embryogenesis. Our current understanding of the molecular circuitry underlying neural induction was influenced by the observation that inhibition of ongoing TGFβ signaling through molecular interference or cell dissociation, rather than the activation of any signaling pathway, is sufficient to establish a neural fate in amphibian embryos. These observations led to the articulation of the "default model" of neural induction [2, 3], which posits that: (a) conversion of embryonic cells to neural fate requires elimination of TGFβ signaling, (b) this conversion is direct and does not require concomitant induction of mesendodermal fates, and (c) neural tissue defaults to forebrain character [4].

TGFβ signaling is induced by ligand-dependent dimerization and activation of type I and type II serine-threonine kinase receptors, which in turn induce signaling by either the canonical pathway, via receptor-associated SMAD proteins (R-SMADs) or by the noncanonical pathway [5, 6]. R-SMAD2/3 mediates transduction via Activin/Nodal/TGFβ1-3, while R-SMAD1/5/8 transduces signals from Bone morphogenetic protein (BMP) ligands in the canonical branch of TGFβ signaling. Threshold-specific activation of R-SMADs has been shown to regulate cell fate decisions in all embryonic cells. For example, medium R-SMAD2/3 and low R-SMAD1/5/8 thresholds are necessary for the maintenance of the human embryonic stem cell (hESC) pluripotency. Higher threshold activation leads to the induction of mesoderm and endoderm, respectively, for SMAD2/3, and trophectodermal cells for SMAD1/5/8, in hESCs [7, 8]. Inhibition of TGFβ signaling can occur by secreted inhibitors, such as Noggin, Chordin, Follistatin, and Cerberus, or by intracellular inhibitors of signal transduction such as SMAD6 and SMAD7. The default state of neural fate represents maximal inhibition of R-SMAD activity. The fact that secreted inhibitors are localized specifically to the organizer in amphibians during gastrulation and the finding that they biochemically interact to inhibit the activity of TGFβ ligands reconcile conclusions of classic experimental embryology with molecular biology. There is now ample evidence demonstrating that regardless of the level at which inhibition occurs, in the absence of TGFβ signaling, early frog embryonic cells default directly to neural fate of telencephalic character [4].

TGFβ inhibition has also been shown to be sufficient to delineate neural from non-neural ectoderm in *Drosophila* early embryos, demonstrating evolutionary conservation from arthropods to amphibians [9]. Despite this wealth of evidence, the validity of the default model of neural induction has been challenged in amniotes and mammals [10]. Notably, in chick embryos, inhibition of TGFβ signaling has been suggested to be insufficient for neural induction, and instead fibroblast

Author contributions: M.Z.O.: conception and experimental design, data collection and assembly, analysis and interpretation of data, and manuscript writing; S.N.: conception, data collection and assembly, analysis of data, and manuscript writing; A.W.: analysis and interpretation of data; J.E.K.: data collection and analysis; A.H.B.: conception and design, financial support, data assembly, analysis and interpretation, manuscript writing, and final approval of manuscript.

Correspondence: Ali H. Brivanlou, Ph.D., Laboratory of Molecular Embryology, The Rockefeller University, 1230 York Avenue, RRB 735, New York 10065, USA. Telephone: 212-327-8656; Fax: 212-327-8585; e-mail: brvnlou@rockfeller.edu Received March 13, 2012; accepted for publication August 1, 2012; first published online in STEM CELLS *EXPRESS* October 3, 2012.
1066-5099/2012/$30.00/0 doi: 10.1002/stem.1246

growth factor (FGF) signaling has been posited as a requirement [11]. Genetic dissection of neural induction in the mouse has been hampered by the highly redundant activities of node secreted inhibitors. Nevertheless, mouse embryos lacking *Nodal* display a precocious neural conversion of nearly the entire embryo into forebrain tissue [12], and double knockout embryos of *Noggin* and *Chordin* fail to develop anterior neural structures [13]. These observations provide support for the evolutionary conservation of default neural induction in mammalian embryos [10]. However, the complexity of the phenotype induced by the mutations impedes their interpretation with regards to the validity of default model (i.e., for TGFβ inhibition to be sufficient to directly induce telencephalic fate) in mammals.

In the absence of conclusive evidence from genetic analysis of the mouse, ESCs have been recently used to show the requirement of TGFβ inhibition for neural induction in mammals. Several protocols have been developed for neural induction, with most using small molecule inhibitors of the TGFβ pathway [14–17] or simply FGF [18, 19]. However, the interpretation of the early events leading to neural induction in these studies has been complicated by several factors: (a) multiple changes of extrinsic influences in culture conditions, (b) neuralization has not been shown unequivocally to be a result of direct conversion, (c) the character of generated neural tissue is heterogeneous, and (d) in some instances, there is an absence of anterior neural fates. These limitations preclude a definitive conclusion on the relevance of the default model of neural induction in mammalian ESCs.

Among the many inhibitors of TGFβ signaling, SMAD7 is known to be a potent, cell autonomous inhibitory SMAD that functions downstream of receptor activation and can act as a potent neural inducer in *Xenopus* when overexpressed [20, 21]. During development, activation of either Activin/Nodal or BMP pathways can induce SMAD7 transcription in most cells, where it acts as a negative feedback regulator of both these branches [21]. SMAD7 has been shown to be maternally expressed in *Xenopus* and zebrafish embryos and two-cell stage mouse embryos and is maintained throughout early development in both species [20, 22, 23]. Overexpression of SMAD7 at the zygotic stage causes mouse embryos to become developmentally arrested at the two-cell stage [23]. This suggests that regulation of SMAD7 levels might be essential for early developmental events to proceed in the embryo. Indeed, SMAD7 is maintained at low levels in zebrafish embryos and mouse ESCs (mESCs) by the E3 ligase RNF12, which promotes its degradation [24]. mESCs deficient in RNF12 show higher levels of SMAD7 and are resistant to the anti-neuralizing effects of BMP as well as the mesoderm-inducing effects of Activin [24]. In the postimplantation embryo, SMAD7 is expressed in all the germ layers of the epiblast, including the early neuroepithelium [23]. Knockout mouse models of SMAD7 have been developed, but have variable phenotypes depending on the knockout approach used [25–27]. Hence, the exact role of SMAD7 during development remains to be elucidated, and it is likely to differ over time and the tissue type being studied. In line with this, SMAD7 has been shown to be essential for mature myelin formation in the postnatal CNS through inhibition of BMP-SMAD1/5/8 activity [28].

To test rigorously whether the default model of neural induction applies in humans, and to overcome the technical hurdles associated with previous neural induction protocols, we asked if the simple expression of SMAD7 is sufficient for direct neural conversion in hESCs. We demonstrate here that just as in frog embryonic cells, SMAD7 overexpression is sufficient to directly convert hESCs from pluripotency to telencephalic fate. Global and time course transcriptome analysis allowed precise evaluation of transcriptional response elicited by other signaling pathways in response to SMAD7 expression and TGFβ inhibition, specifically suggesting the lack of requirement for FGF-MEK signaling in human neural induction. As anticipated, MEK inhibition significantly accelerated telencephalic neural conversion under pluripotency conditions. FGF-MEK and TGFβ-SMAD signaling cooperatively maintain hESCs by promoting pluripotency genes and repressing neural genes [29–31]. Our findings suggest that in the absence of these cues, pluripotent cells simply revert to a program of neural conversion; hence, the "primed" state of hESCs requires inhibition of the "default" state of neural fate acquisition. Our study thus demonstrates an evolutionary conservation of the default pathway of neural induction from frogs to humans.

Materials and Methods

Cloning of the ePiggyBac-Inducible SMAD7/EGFP Cassette

Two transposable elements were constructed (Fig. 1A). In the first, a bicistronic cassette encoding EGFP and human SMAD7 separated by T2A sequence was cloned downstream of an inducible Tetracycline response element (TRE) promoter. In the second, constitutively active SV40 and Chicken actin globin (CAG) promoters drive the expression of Hygromycin (Hyg) and the reverse transactivator (rTA-M2), respectively. Following translation, EGFP is cleaved from SMAD7 by virtue of the self-cleaving peptide.

Cell Culture and Neural Induction

The RUES1 and RUES2 hESCs lines were derived in our lab and have been described previously [32, 33]. ESCs were maintained in feeder-free conditions on Matrigel (BD Biosciences, San Jose, CA)-coated dishes and cultured in conditioned medium (CM). For microarray and quantitative PCR (qPCR) experiments, mTESR (Stem Cell Technologies, Vancouver, Canada) was used as the culture medium. Whenever mTESR was used, hESC cultures were adapted to the medium for at least two to three passages prior to SMAD7 induction with doxycycline (DOX). For the preparation of CM, mitotically inactivated mouse embryonic fibroblasts were seeded at a density of 1.0×10^7 cells per 150-mm dish and incubated in knockout serum-replacement (KSR) medium (Dulbecco's modified Eagle's medium supplemented with 20% KSR, 100 μM nonessential amino acids, 2 mM GlutaMAX, 100 μM β-mercaptoethanol, 100 U/ml penicillin, 100 μg/ml streptomycin, and 1× B27 supplement; all from Life Technologies, Grand Island, NY) with 20 ng/ml basic FGF (bFGF) for 24 hours. CM was collected and supplemented with 20 ng/ml bFGF prior to feeding the hESCs. For expansion, hESCs were grown as colonies and enzymatically passaged with 1 mg/ml dispase. For neural conversion, clonal RUES1-SMAD7 hESCs (see below) were pretreated for 1 hour with 10 μM ROCK-inhibitor (Y-27632; Tocris, Minneapolis, MN) and passaged as single cells with TrypLE Express (Life Technologies, Grand Island, NY). ROCK-inhibitor strongly diminishes dissociation-induced apoptosis and increases cloning efficiency [34]. The cells were subsequently plated onto Matrigel-coated wells at a density of 15,000–30,000 cells per square centimeter in CM supplemented with ROCK-inhibitor and Hyg for 3 days, after which DOX (2 μg/ml; Life Technologies, Grand Island, NY) was added to the medium (supporting information Fig. S2). This was considered Day 0 of induction. Media were replaced every day with DOX for the duration of the experiment; DOX was excluded for the control wells. For the MEK-I experiments, the cells were seeded onto Matrigel-coated wells as before, and MEK-I was added at various time points as indicated in the text. For BMP4/TGFβ1-challenge experiments, the cells were passaged in dispase and seeded as colonies. Where applicable, the TGFβ inhibitor SB431542

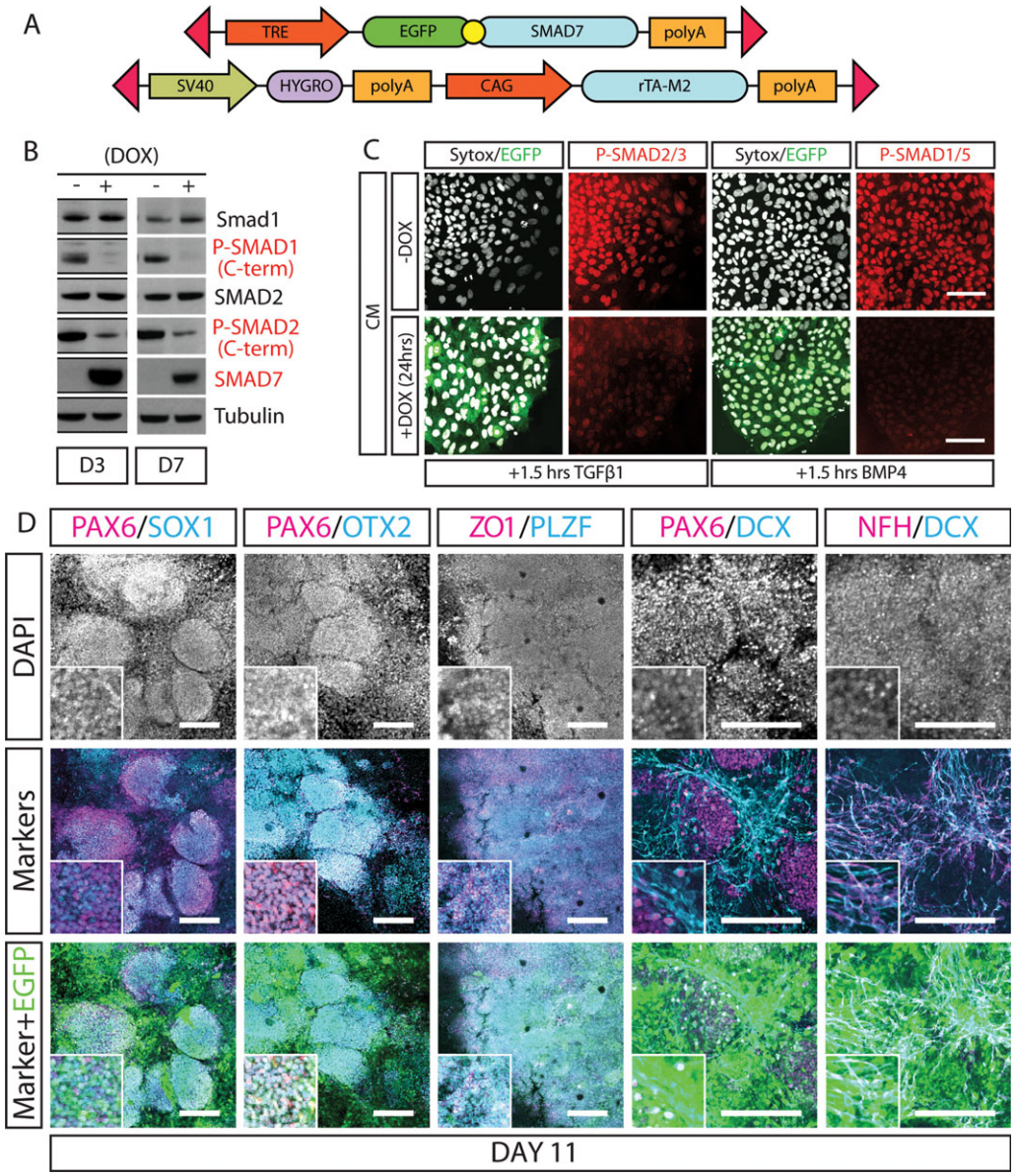

Figure 1. SMAD7 induction promotes neural conversion of human embryonic stem cells (hESCs) via inhibition of Activin/Nodal and BMP signaling in hESCs. **(A):** Schematic of the ePiggyBac constructs used to create the SMAD7 cell line from RUES1 hESCs. The ePB-HYGRO-CAG-rTA/M2 codes for a tetracycline transactivator that binds to the TRE promoter sequence in ePB-TRE-EGFP-T2A-SMAD7 only in the presence of DOX and permits inducible SMAD7 expression. The T2A peptide enables post-translational cleavage of SMAD7 from EGFP. **(B):** Western blots show loss of C-terminal phosphorylation—and hence activity—of SMAD1 and SMAD2 in RUES1-SMAD7/EGFP cultures on DOX induction on Days 3 and 7. Note the tightly regulated expression of SMAD7. **(C):** Immunocytochemistry confirms attenuation of SMAD2/3 and SMAD1 C-terminal phosphorylation in SMAD7-induced cultures on exposure to high doses of BMP4 and TGFβ1. RUES1-SMAD7/EGFP cultures were induced with DOX for 24 hours, challenged with 25 ng/ml TGFβ1 and 50 ng/ml BMP4 for 1.5 hours, and subsequently fixed. These experiments were carried out in CM. Sytox is used here as a nuclear counterstain. **(D):** Immunofluorescence microscopy reveals extensive expression of the neural determinant PAX6 on Day 11 under pluripotency conditions. Strong colocalization of PAX6 with another neural-specific gene SOX1 is also observed, while near-complete overlap is seen with the anterior gene OTX2. The morphology of cells at this stage is largely that of prerosette neuroepithelia, as revealed by even distribution of ZO1 on the cell surface. The neural enriched transcription factor PLZF is also expressed at this stage. Clusters of PAX6+ cells are surrounded by migratory DCX+ neurons. NFH+ cells with features of mature neurons are also seen in areas of DCX+ cells. Insets show representative higher magnification views of the differentiated cells. Scale bars represent 200 μm. Abbreviations: CM, conditioned medium; DAPI, 4',6-diamidino-2-phenylindole; DCX, doublecortin; DOX, doxycycline; EGFP, enhanced green fluorescent protein.

(Stemgent, Cambridge, MA), the BMP inhibitor LDN193189 (Reagents Direct, Encinitas, CA), and the MEK-inhibitor PD0325901 (Tocris, Minneapolis, MN) were used at concentrations of 10 μM, 100 nM, and 1 μM, respectively. BMP4 and TGFβ1 (both from R&D Systems, Minneapolis, MN) were used at concentrations of 50 ng/ml and 25 ng/ml, respectively. Media were replenished daily in all conditions.

Generation of Transgenic Cell Lines

RUES1 and RUES2 cultures were pretreated for 1 hour with 10 μM ROCK-inhibitor and dissociated with 0.05% Trypsin. The cells were then washed in CM with ROCK-inhibitor and resuspended in nucleofection solution L (Lonza, Basel, Switzerland). The helper transposase, ePB-HYGRO-CAG-rTA-M2, and ePB-

TRE-SMAD7-T2A-EGFP plasmids were added to the cell suspension (Fig. 1A), and nucleofection was performed with program setting B-016 as described [35]. The transfected cells were then plated on Matrigel in CM supplemented with 10 μM ROCK-inhibitor. The inhibitor was removed after 24 hours and colonies were allowed to form over the next several days. Hyg (200 μg/ml; Life Technologies, Grand Island, NY) was initiated 3 days after nucleofection and maintained for approximately 10 days until large resistant colonies became visible. For selection of a clonal RUES1-SMAD7/EGFP line, 10 Hyg-resistant colonies were picked manually and grown on feeder layers in CM. Each colony-derived culture was subsequently split into two 24-well plates. One plate was induced with 2 μg/ml DOX while the other was maintained without DOX. The clonal lines displaying uniform EGFP expression in the induced plates were chosen for subsequent experiments from the uninduced plate. Strict Hyg selection was maintained in the culture medium up until the day before DOX induction. Similar protocols were followed for derivation of the RUES2-SMAD7/EGFP line, except that clonal selection was not carried out. Extended materials and methods are provided in supporting information available on the Stem Cells website.

RESULTS

SMAD7 Inhibits TGFβ Signaling and Induces a Neural Fate in hESCs

SMAD7 mRNA injections are sufficient to directly induce telencephalic fate in *Xenopus* pluripotent embryonic cells [20]. In order to address whether increasing SMAD7 levels could also completely inhibit TGFβ signaling and convert hESCs to neuroepithelia, we used the ePiggyBac transposon system [35] to generate a Tet-inducible bicistronic expression cassette encoding EGFP (used as lineage tracer), attached to human SMAD7 via self-cleaving peptide sequence (Fig. 1A). A second construct constitutively expressing Hyg resistance and reverse transactivator (rTA-M2) was also generated. These constructs, along with a plasmid encoding the transposase, were transfected into an hESC line, RUES1 [36], and grown in Hyg selection. A Hyg-resistant clonal line called RUES1-EGFP/SMAD7 was isolated and further expanded. Addition of DOX led to the EGFP expression (Fig. 1C, 1D; supporting information Fig. S1A) as well as strong induction of SMAD7 compared to endogenous SMAD7 as determined by Western blot (Fig. 1B).

After 48 hours of induction, the cells displayed marker changes consistent with exit from pluripotency as observed by the decreases in OCT4 (see below) and undetectable NANOG expression (supporting information Fig. S1A). As the SMAD2 branch of the TGFβ pathway has been shown to be necessary for the maintenance of hESC pluripotency [31, 32], exit from pluripotency was consistent with SMAD7-inhibition of Activin/Nodal signaling. Activation of R-SMADs occurs by C-terminal phosphorylation of serine residues and nuclear translocation. Functional analysis confirmed that SMAD7 was indeed inhibiting R-SMADs by preventing C-terminal phosphorylation as determined by Western blot (Fig. 1B). Immunofluorescence (IF) confirmed that SMAD7-induced hESCs were resistant to R-SMAD C-terminal phosphorylation in the presence of TGFβ1 and BMP4 ligands (Fig. 1C; supporting information Fig. S1A) [7, 8]. In addition, SMAD7-induced cells failed to upregulate the trophectodermal marker CDX2 in response to BMP4 after 48 hours of DOX induction and did not show morphological changes of trophectodermal differentiation, whereas it could be readily detected in uninduced BMP4-treated cells (supporting information Fig. S1A). These results establish that in hESCs, SMAD7 expression inhibits TGFβ signaling biochemically and functionally.

Examination of the induced cells by cell type-specific markers demonstrated induction of neural markers at Day 11 such as PAX6, OTX2, SOX1, and NFH (Fig. 1D). A marker of migratory neurons, doublecortin (DCX) was also demonstrable at this time point (Fig. 1D). Flow cytometric quantification of PAX6 demonstrated that at Day 11, approximately 97% of the EGFP-positive RUES1-SMAD7/EGFP cells had adopted a neural fate (Fig. 3A). We were able to confirm expression of these markers and efficient induction of PAX6 in an independent RUES1-SMAD7/EGFP clone, as well as another SMAD7-expressing hESC line, RUES2-SMAD7/EGFP (supporting information Fig. S7C). As induction of neural fate occurred by simple addition of DOX to the pluripotency culture medium, without the requirement of any other changes in extrinsic factors, this initial experiment establishes that SMAD7 induction was sufficient for neural conversion under these conditions. This was comparable to that seen with small molecule inhibitors of ALK receptors using the published "dual-SMAD inhibition" protocol [14] (supporting information Fig. S7B), suggesting that SMAD7-mediated inhibition of Activin/Nodal-SMAD2/3 and BMP-SMAD1/5/8 signaling is the primary mechanism of action. Lastly, SMAD7-generated neuroepithelium could also generate glia at later stages, as determined by the astrocyte marker glial fibrillary acidic protein (supporting information Fig. S7A).

Timing of SMAD7-Mediated RUES1 Neural Induction

To determine the exact timing of conversion from pluripotency to neural fate, time course microarray studies at discrete time points following SMAD7 induction were performed in parallel with IF of cell type-specific molecular markers (supporting information Fig. S1B). Transcriptome analysis of induced RUES1-EGFP/SMAD7 transgenic cells was done every day for 7 days, and at three time points during the first day (6, 12, and 24 hours), and analyzed relative to uninduced controls. Parallel confocal IF studies were extended to Day 17 (supporting information Fig. S1B).

Time course heatmaps showed that at the transcriptional level, the expression of a panel of molecular markers of pluripotency [37] including NANOG, OCT4, DMNT3B, ETS1, BAMBI, GDF3, ZFP42, and LEFTY2 were downregulated by Day 1–2, and were lost after 1 week of DOX induction (Fig. 2A; supporting information Table S3). This was independently confirmed by qPCR for OCT4 and NANOG (Fig. 2C) and by IF for OCT4 (Fig. 2D). Interestingly, we also observed transient upregulation of the epiblast marker ZIC2 (Day 3) and a sustained upregulation of the epiblast and anterior neural fold marker POU3F1 (data not shown), as has been reported for mouse embryos in vivo and mESCs in vitro [38]. This suggests that even though hESCs share defining characteristics with mouse epiblast stem cells (mEpiSCs) [39], they still pass through a primitive ectoderm phase during neural conversion. The decline of pluripotency gene expression coincided with the gradual expression of early neural markers, including OTX2, PAX6, NR2F2, POU3F1, HES5, HESX1, SIX3, DACH1, ZNF521, and SIP1, which were induced at days 2–5 (Broad Molecular Signature Database; Figs. 2B, 4E; supporting information Table S3). In addition, downregulation of more mature neuronal markers was also observed in this time window (Fig. 2B; supporting information Table S3). Expression of PAX6 and SOX1 was confirmed independently by qPCR (Fig. 2C). IF for PAX6, SOX1, and neural cell adhesion molecule (NCAM) (Figs. 2E, 2F, 3C), and flow cytometry

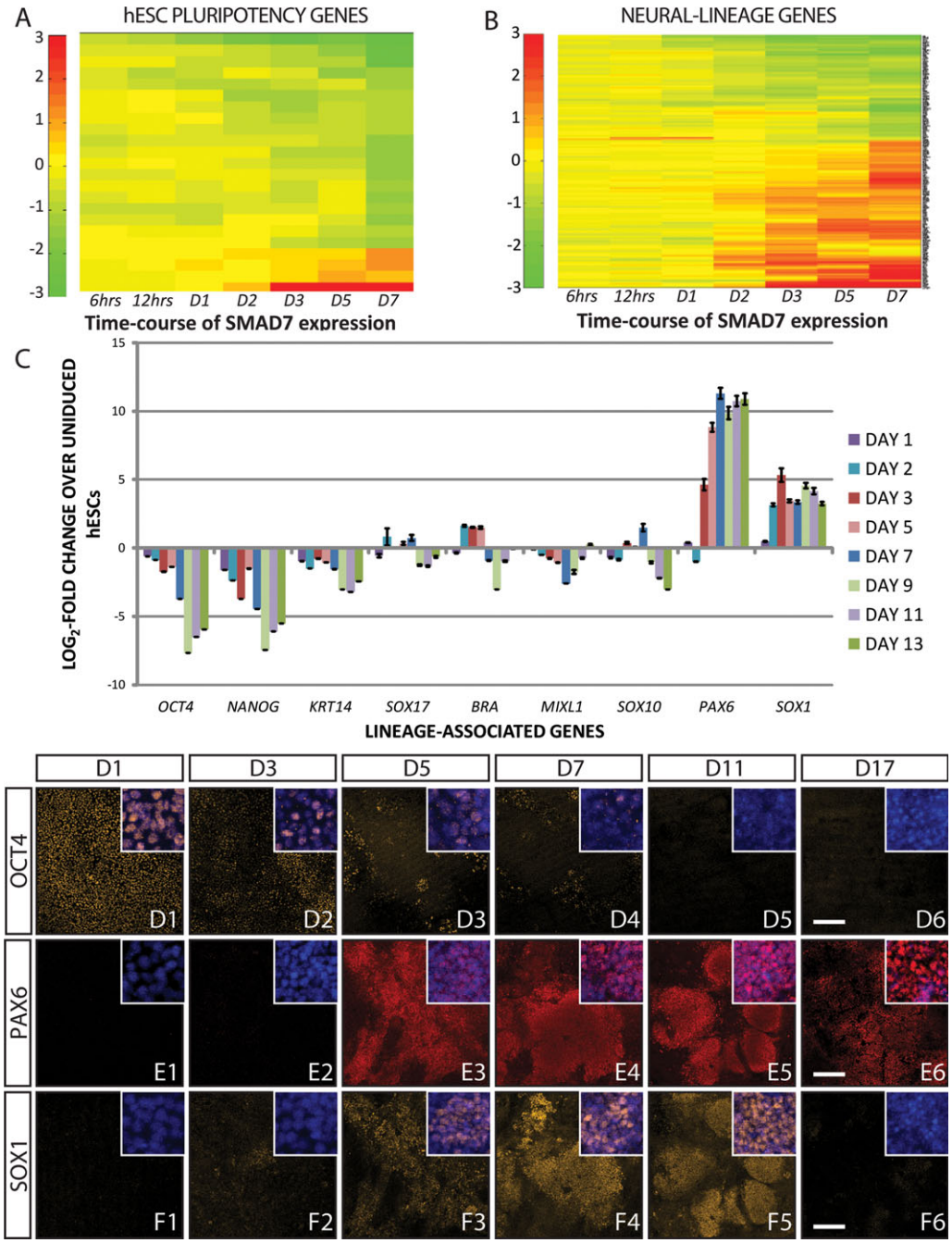

Figure 2. SMAD7 is sufficient for neural conversion of hESCs under conditions favoring pluripotency without contamination by non-neural lineages. **(A):** Heatmap of pluripotency genes changing by more than or equal to twofold on SMAD7 induction under pluripotency conditions. The pluripotency gene list was derived from Suarez-Farinas et al. and Boyer et al.; the complete list of genes in the order presented can be found in Supporting Information Table S3. **(B):** Time course heatmap from global transcriptome analysis of SMAD7-induced cultures showing gradual acquisition of a neural fate. Genes upregulated or downregulated by more than or equal to twofold are shown. The complete list of genes in the order presented can be found in Supporting Information Table S3. **(C):** Quantitative PCR (qPCR) of various lineage-specific genes from Days 1 to 13 of DOX induction. A decrease in transcripts of pluripotency genes (OCT4 and NANOG) and absence of ectodermal (KRT14), neural crest (SOX10), endodermal (SOX17), or mesodermal (BRA, MIXL1) lineage transcripts is observed. The small upregulation of BRA between Days 2 and 5 was not accompanied by nuclear localization of the protein on immunofluorescence (Supporting Information Fig. S5A, S5B). Strong upregulation of PAX6 is also seen. Time course expression of neural and pluripotency markers between Days 1 to 17 in SMAD7-induced cultures are shown in **(D--F)**. Insets in (D--F) show representative higher magnification views. The nuclear counterstain (DAPI) is pseudocolored blue. (D): Panels D1-D6 show that the pluripotency marker OCT4 is strongly downregulated at Day 3 and completely disappears by Day 11. (E): As shown in panels E1-E6, expression of PAX6 is first observed on Day 5 and persists till Day 17. (F): PAX6 expression is paralleled by expression of another early neuroepithelial gene SOX1, which decreases by Day 17 (panels F1-F6). Between days 3 and 11, there is a strong overlap between domains of PAX6 and SOX1 expression. qPCR data are presented as LOG_2-fold change over uninduced hESCs. ATP5O was used for internal normalization at each time point. Bars represent $n = 3–4 \pm$ SEM. Scale bars represent 200 μm. Abbreviations: DAPI, 4',6-diamidino-2-phenylindole; hESCs, human embryonic stem cells.

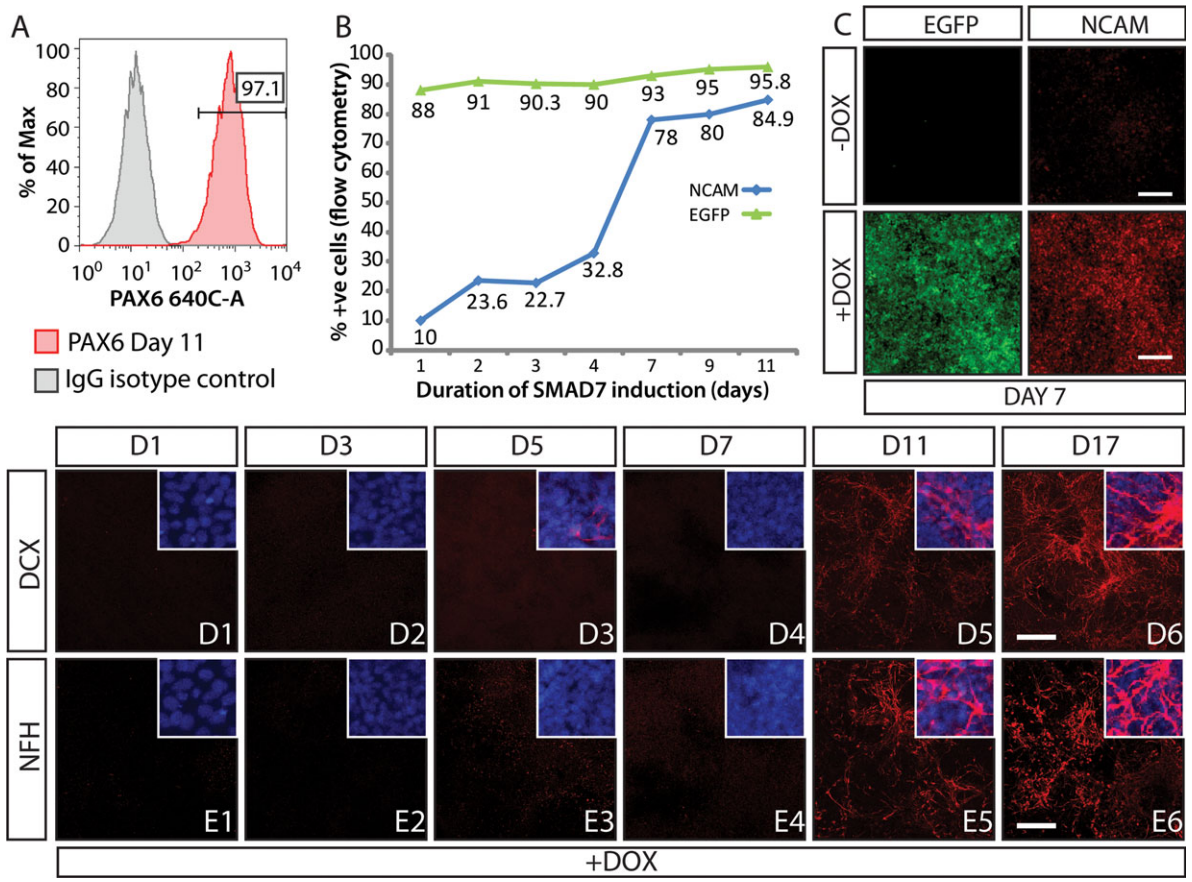

Figure 3. Efficient neuralization in SMAD7-induced hESCs under conditions favoring pluripotency. **(A):** Flow cytometry histogram of EGFP+ cells showing that majority of SMAD7-induced cells become PAX6+ by Day 12 of induction under pluripotency conditions. **(B):** Dynamics of neural cell adhesion molecule (NCAM) expression on DOX induction as determined by flow cytometry. Approximately 85% of EGFP+ cells is also NCAM+ by Day 7, and this correlates with PAX6 expression observed by immunofluorescence (IF) (Fig. 3F). NCAM+ cells comprise approximately 90% of EGFP+ cells on Day 11. **(C):** IF of SMAD7-induced cultures selectively expressing the surface marker NCAM (CD56) on Day 11 of DOX (lower panels). Almost complete colocalization with EGFP+ cells is seen. A few NCAM+ cells are also seen in uninduced cultures (upper panels). **(D):** Time course analysis of differentiating SMAD7-induced cells shows that the migrating neuronal marker DCX, a marker of early neuronal differentiation, is observed Day 11 onwards (panels D1-D6) in cells with clear neuronal morphology. **(E):** The postmitotic neuronal marker NFH is also observed in these cultures at later time points (panels E1-E6). While colocalization of DCX and NFH as well as PAX6 and DCX was seen in some areas, they are largely mutually exclusive (Fig. 1D). EGFP expression is not shown here for simplicity. Scale bars represent 200 μm. Insets in (D) and (E) show representative higher magnification views. The nuclear counterstain (DAPI) is pseudocolored blue. Abbreviations: DCX, doublecortin; DOX, doxycycline; EGFP, enhanced green fluorescent protein; hESCs, human embryonic stem cells; NFH, neurofilament H.

for the pan-neural marker NCAM (Fig. 3B) also supported the gradual acquisition of neural fate by the SMAD7-expressing cells. Flow cytometric quantification of PAX6 demonstrated that at Day 11, the majority (97%) of the EGFP-positive cells had adopted a neural fate (Fig. 3A). In addition, expression of markers of more differentiated cells was readily detectable by IF at Day 5 for NCAM and Day 7 for DCX and NFH (Fig. 3C--3E). Taken together, the results from time course microarray, qPCR, and IF demonstrate that SMAD7-mediated neural induction in RUES1-EGFP/SMAD7 starts after 3 days post-DOX induction in feeder-free pluripotency conditions with high levels of FGF signaling.

The dynamics of expression of these transcription factors support the specificity of SMAD7 in inhibiting the Activin/Nodal-SMAD2/3 and BMP-SMAD1/5/8 branches. In addition, it also provides an insight into how SMAD7 can promote neural induction. It is known that Activin/Nodal-SMAD2/3 signaling maintains pluripotency in hESCs by directly maintaining expression of NANOG [40]. NANOG in turn forms a core pluripotency circuitry with OCT4 and SOX2 by binding to the promoters of each other in a feed-forward loop [41]. Additionally, NANOG, OCT4, and SOX2 together bind to the promoters of and repress many differentiation-specific genes in ESCs. Inhibition of Activin/Nodal-SMAD2/3 by SMAD7 downregulates NANOG and by doing so promotes expression of the zinc finger homeodomain transcription factor ZEB2 (SIP1) [29], as shown here by qPCR and microarray data (Fig. 4A, 4E). ZEB2 has previously been shown to promote neuroectodermal differentiation and prevent mesendodermal differentiation of hESCs [29]. In addition, SMAD7 also promotes induction of OTX2 and NR2F2 (Fig. 4B, 4E), which are among the earliest transcription factors expressed during neural differentiation of hESCs [30, 42]. OTX2 can bind to and directly activate transcription of the neural determinant PAX6 [30] in hESCs. Likewise, in early neuroepithelium, NR2F2 represses OCT4 expression directly and promotes expression of other neural-specific markers [42]. In pluripotent hESCs, OCT4 and the OCT4-induced microRNA mir-302 repress NR2F2 expression by transcriptional and post-transcription mechanisms, respectively. Inhibition of BMP-SMAD1/5/8 branch by SMAD7 is probably contributing to neuroectodermal differentiation through several mechanisms

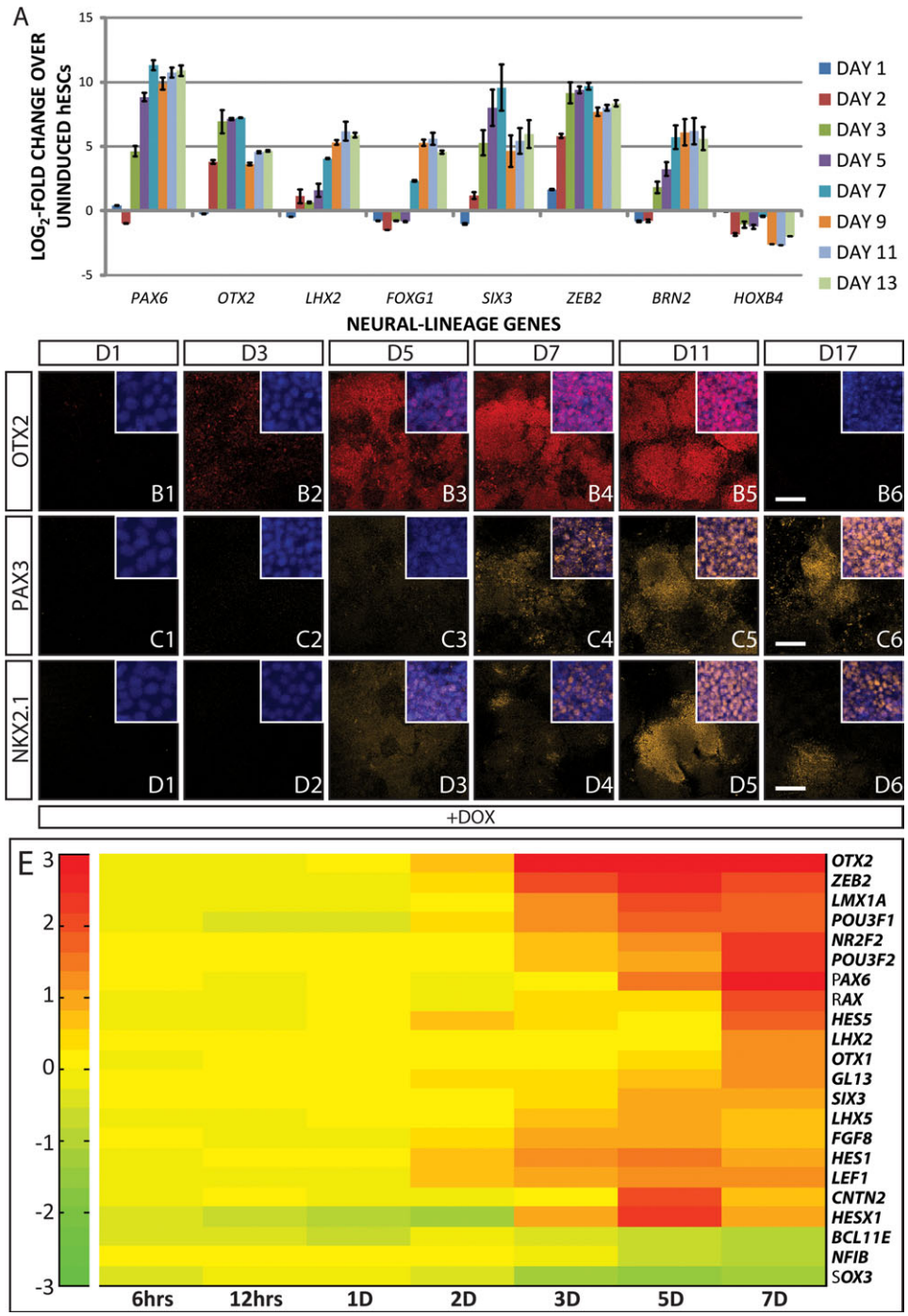

Figure 4. SMAD7 imposes an anterior identity in neuralized hESCs. **(A):** Quantitative PCR (qPCR) of neural lineage genes from Days 1 to 13 of DOX induction. A robust increase in neural lineage transcripts such as SIP1, SOX1, and BRN2 as well as anterior neural transcripts such as OTX2, SIX3, LHX2, and FOXG1 is seen. Primers specific to the anterior neural-specific isoform of OTX2 were used. Downregulation of the hindbrain transcript HOXB4 is also observed. Time course expression of dorsal and ventral forebrain markers between Days 1 and 17 in SMAD7-induced cultures are shown in **(B--D)**. hESCs were induced in conditions favoring pluripotency as before. (B): The first marker upregulated is the anterior marker OTX2 (panels B1-B6). Near complete colocalization of OTX2 is seen with PAX6 from Day 5 onwards (Fig. 1D), suggesting a neural, rather than anterior visceral endodermal source of expression of OTX2. (C): The dorsal neural tube marker *PAX3* is also seen in the cultures between Days 5 through 17 (panels C1-C6). During mouse development, *PAX3* is expressed in some parts of the dorsal forebrain early on. (D): Clusters of cells expressing the ventral telencephalic (medial ganglionic eminence) marker NKX2.1 are also observed in the cultures in a mutually exclusive manner to PAX6 (panels D1-D6). **(E):** Time course heatmap from global transcriptome analysis showing expression of genes associated with forebrain signature. Genes upregulated or downregulated by more than or equal to twofold are shown. The complete list of genes in the order presented can be found in Supporting Information Table S3. qPCR data are presented as LOG_2-fold change over uninduced hESCs. ATP5O was used for internal normalization at each time point. Bars represent $n = 3–4 \pm$ SEM. Scale bars represent 200 μm. Insets in (B)--(D) show typical high magnification views with nuclear counterstain (DAPI) in blue. Abbreviations: DAPI, 4',6-diamidino-2-phenylindole; DOX, doxycycline; hESCs, human embryonic stem cells.

as well. First, it promotes the specificity of neural induction by inhibiting induction of non-neural germ layers [30], as shown below. Indeed, inhibition of BMP signaling together with downregulation of OCT4 is a prerequisite for neuroectodermal specification in hESCs [43]. Second, inhibition of BMP signaling may serve to stabilize the neural program by maintaining expression of shared pluripotency and neural genes such as SOX2 [30], and this is also observed in our microarray analysis. Third, absence of BMP signaling promotes expression of cell-intrinsic neural determinants, such as the zinc finger transcription factor ZNF521, which is necessary and sufficient for neural induction in hESCs [38]. ZNF521 was also strongly induced under SMAD7 induction at Day 11 (Fig. 5E and data not shown).

SMAD7-Mediated Neural Induction in hESCs Is Direct

Pluripotent cells can adopt a neural fate by either direct or secondary/concomitant induction of other embryonic germ layers such as mesoderm, organizer/node, endoderm, or extra-embryonic tissue. To address whether SMAD7-mediated neural conversion was direct, we analyzed the microarray dataset, which indicated that DOX-induced RUES1-EGFP/SMAD7 did not express markers of other embryonic germ layers at any time point (data not shown). These included Brachyury (BRA), MIXL1, and HAND1, for mesoderm; SOX17, GATA4, or GATA6, for endoderm; CDX2, EOMES, β-HCG, and KLF5, for trophectoderm; and KRT14 for non-neural ectoderm. This conclusion was independently confirmed by qPCR for BRA and MIXL1 for mesoderm and SOX17 for endoderm (Fig. 2C) and by IF for BRA and SOX17 (supporting information Fig. S5A, S5B, S5E). In addition, SMAD7-induced cells did not express markers of the non-neural ectoderm marker (skin) KRT14 or the neural crest progenitor marker SOX10, as determined by qPCR. Importantly, SMAD7 did not induce expression of organizer/node-specific markers such as GSC, MIXL1, FOXD3, or FOXA2 (also demarcating the floor plate at later time points) [44], demonstrating that neural fate induction was not following or concomitant with the formation of an organizer/node. These results provide evidence for direct induction of neural fate from pluripotent hESCs and support the validity of the second attribute of the default model: direct conversion from pluripotency to neural fate.

Neural Tissue Induced by SMAD7 Is Telencephalic in Identity

Finally, we addressed the character of SMAD7-induced neural fate globally in function of time followed by independent confirmation with qPCR and IFs. We first looked at the anteroposterior identity of the induced neural tissue. Microarray data indicated the presence of the most anterior neural fate in SMAD7-induced cells, as evidenced by expression of the anterior-specific neural genes such as OTX1/2, SIX3, LHX2, ZNF521, LHX5, SP8, LIX1, LMO4, RAX, SIX6, and GLI3 (Fig. 4A, 4E; supporting information Table S3). This was also confirmed by Gene Ontology analysis for over-represented genes on Day 7 (supporting information Fig. S3). Induction followed a temporal hierarchy. For example, genes induced by at least fivefold by DOX included OTX2 and ZEB2, first induced at Day 2, PAX6 and SIX3 at Day 3, LHX2 and FOXG1 at Day 7, and BRN2 (POU3F2) at later time points. Early expression of OTX2 was confirmed by IF (Fig. 4B). However, no markers of midbrain (EN2), hindbrain, and spinal cord (HOXB4) were detected at any time point, suggesting specific induction of human telencephalic fate (Fig. 4A; supporting information Fig. S5E, S5F). Importantly, we also did not observe significant induction of the neural crest stem cell marker SOX10 (Fig. 2C; supporting information Fig. S2C, S2D). Examination of dorsal-ventral markers established the presence of both dorsal and ventral cell types within the forebrain territory, as demonstrated by the expression of PAX6 and *PAX3* [45] (Fig. 4C). Surprisingly, while ventral fate, such as medial ganglionic eminence, was detected in some clusters delineated by NKX2.1 expression (Fig. 4D), the most ventral fate (floor plate) did not seem to be induced (data not shown). Together, these results establish that the third attribute of the default model—that is, anterior neural conversion—is also valid in hESCs, as in frogs, and supports the notion that the molecular circuitry underlying early neural induction is evolutionarily conserved in humans.

Inhibition of FGF-MEK Signaling Promotes SMAD7-Mediated Neural Fate

FGF-MEK signaling is required for the maintenance of pluripotency through NANOG expression in hESCs [46], but not mESCs. Additionally, the FGF-MEK signaling pathway has been proposed to be required for mammalian neural induction [47, 48]. Due to the requirement of FGF and Activin/Nodal signaling for maintenance of the pluripotent state of hESCs, it has been suggested that hESCs represent an epiblast-like state rather than the ICM state of mESCs. Furthermore, a brief exposure of FGF-MEK signaling is required for mESC to become epiblast cells, which can then be grown in the presence of Activin, like their hESC counterparts [39]. For mESC neural induction, FGF might be required initially simply to allow the transition of mESCs to an epiblast fate, but not later for neural induction [49, 50].

In order to obtain high-resolution views of the secondary signaling events operating downstream of SMAD7-mediated neuralization, we analyzed genes pertaining to the developmentally relevant signaling pathways in our time course microarray (supporting information Fig. S4A--S4F; supporting information Table S3). Interestingly, we found an overall downregulation in many components of FGF/MAPK signaling and upregulation of several cell-intrinsic inhibitors of MAPK signaling in our analysis (Fig. 5A; supporting information Fig. S4B, S4F; supporting information Table S3). These inhibitors included the dual-specificity phosphatase inhibitor (*DUSP4*), the cell-intrinsic FGF, and WNT inhibitors of the SHISA family (*SHISA2* and *SHISA3*) as well as a FGF/EGF cell-intrinsic inhibitor of the SPROUTY family (*SPRY1*). We followed up on these observations to address the relevance of FGF-MEK signaling in hESC neural induction. FGF-MEK signaling was inhibited using the specific MEK1/2-inhibitor PD0325901 (MEK-I) to block the pathway downstream of the receptor under pluripotency conditions. MEK-I was added to RUES1-SMAD7/EGFP cultures at 0, 12, 24, and 48 hours after DOX induction, and cells were cultured in the presence of the inhibitor until Day 7 of DOX induction. No discernible differences in neural conversion were detected between these conditions as determined by PAX6 and OCT4 IF on Day 7 (Fig. 5C), excluding the possibility of MEK1/2 signaling involvement in the epiblast-like transition or neural conversion during this period of hESC differentiation.

The dynamics of neural induction were then determined by combined MEK inhibition and SMAD7 induction in hESCs. We used the small molecule MEK-I at a concentration that can eliminate MEK/ERK phosphorylation in hESCs as determined by Western blot and protein arrays (data not shown). RUES1-SMAD7/EGFP cells were cultured in pluripotency conditions and subsequently treated with MEK-I, DOX, and MEK-I/DOX combinations. cDNA was generated from cells after 0, 1, 3, 5, and 7 days of treatment. qPCR

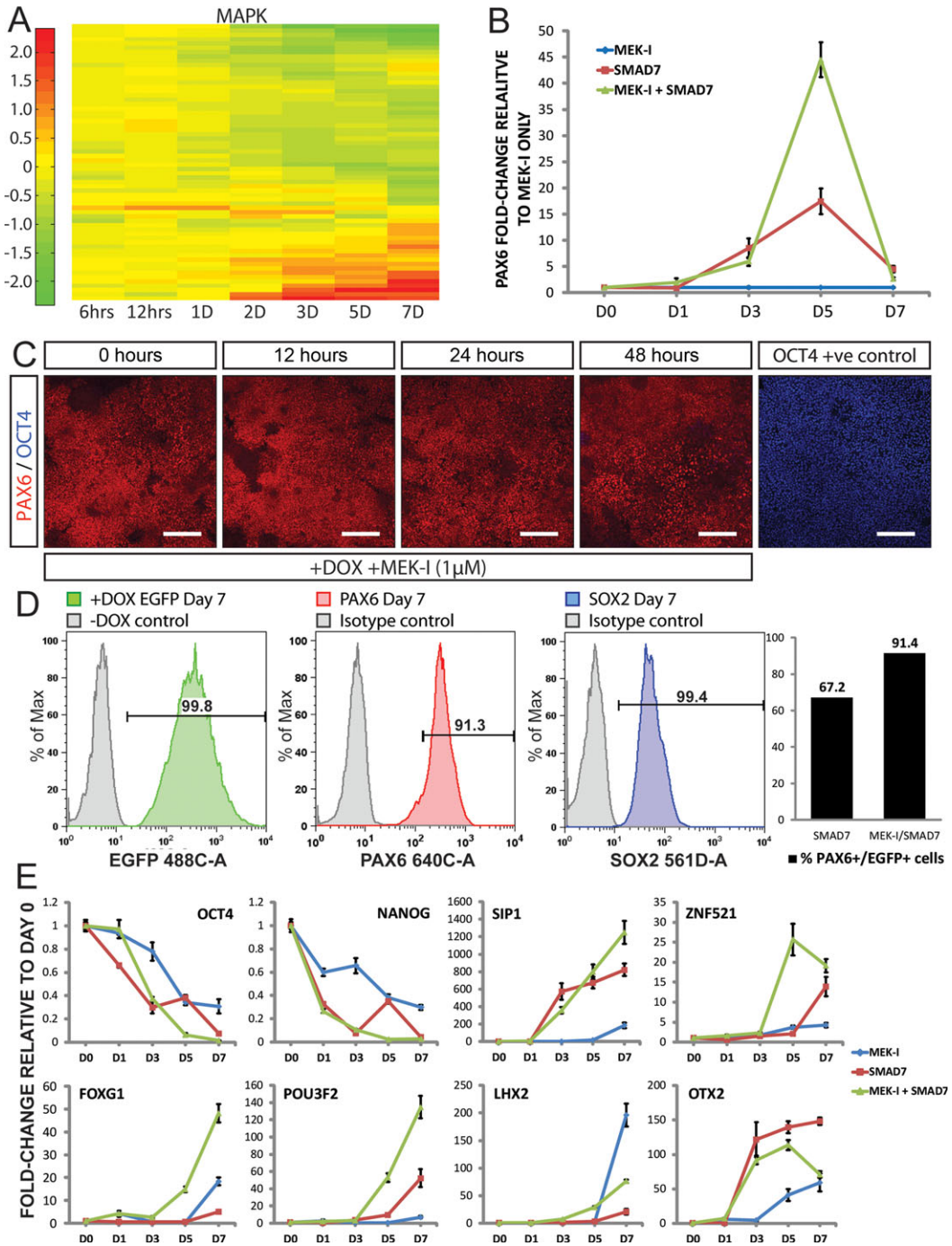

Figure 5. MEK inhibition promotes SMAD7-mediated neural conversion under conditions favoring pluripotency. **(A):** Time course heatmap of the MAPK pathway in induced human embryonic stem cells (hESCs) showing downregulation of several MAPK related genes and upregulation of cell-intrinsic MAPK inhibitors. Genes changing by more than or equal to 1.5-fold are shown on this heatmap. The complete list of genes in the order presented can be found in Supporting Information Table S3. **(B):** Quantitative RT-PCR for PAX6 transcripts in MEK-I (blue), SMAD7 (red), and MEK-I/SMAD7 (green) combinations in pluripotency conditions. MEK-I/SMAD7 and SMAD7 result in significantly higher increase in PAX6 expression relative to MEK-I alone, with the MEK-I/SMAD7 combination leading to a more than threefold increase in PAX6 on Day 5 compared to SMAD7. Quantitative PCR (qPCR) data are presented as relative fold change over MEK-I-treated hESCs. **(C):** MEK inhibition before primitive ectodermal transition does not prevent neural conversion in SMAD7-induced cultures. Addition of MEK-I at 0, 12, 24, and 48 hours after SMAD7 induction did not result in observable differences in PAX6 expression or downregulation of OCT4 on Day 7 of induction. The time labels above the figures represent the time of addition of MEK-I after DOX induction. **(D):** Flow cytometry for EGFP, PAX6, and SOX2 in the MEK-I/SMAD7 combination shows that >90% of the cells are positive for these markers by Day 7 of induction in conditions favoring pluripotency. SOX2 is expressed in both pluripotent cells as well as neuroepithelial cells. **(E):** qPCR of anterior neural genes between Days 1 and 7 of MEK-I (blue), SMAD7 (red), and MEK-I/SMAD7 (green) combinations. Transcripts for anterior neural genes FOXG1, LHX2, ZNF521, BRN2 (POU3F2), and SIP1 are all significantly higher in the MEK-I/SMAD7 combination compared to SMAD7 alone. Downregulation of the pluripotency genes OCT4 and NANOG is more robust in this combination than MEK-I alone. qPCR data are presented as LOG_2-fold change over uninduced hESCs unless otherwise specified. ATP5O was used for internal normalization at each time point. Bars represent $n = 3–4 \pm$ SEM. Scale bars represent 200 μm. Abbreviations: DOX, doxycycline; EGFP, enhanced green fluorescent protein; MAPK, mitogen activated protein kinase.

demonstrated that PAX6, ZNF521, SIP1, and POU3F2 expression increased to significantly higher levels in the MEK-I/SMAD7 condition compared to SMAD7 only and MEK-I only conditions (Fig. 5B, 5E). While PAX6 transcripts were induced by MEK-I alone (data not shown), the other neural determinants SIP1, ZNF521, and POU3F2 were not induced in this condition (Fig. 5E). Furthermore, while downregulation of the pluripotency transcripts OCT4 and NANOG was also seen in MEK-I alone, SMAD7 and MEK-I/SMAD7 conditions demonstrated a more robust downregulation of these transcripts (Fig. 5E). Compared to SMAD7 only, MEK-I/SMAD7 condition showed higher levels of PAX6 (three-folds), the intrinsic neural determinant ZNF521 (25-folds), and the neural POU-domain transcription factor POU3F2 (six-folds) on Day 5, comparable levels of the neural fate determinant SIP1, and an almost complete loss of NANOG and OCT4 expression during this time. Intracellular flow cytometry on Day 7 of the MEK-I/SMAD7 combination for the neural genes PAX6 and SOX2 confirmed expression of these factors in >90% of EGFP+ cells compared to 67% of PAX6 cells in the SMAD7-only condition (Fig. 5D). Together, these results demonstrate that MEK-ERK signaling has an inhibitory, rather than an instructive, role in hESC neural induction and points to TGFβ inhibition as sufficient for neural conversion. Since inhibition of MEK alone can directly upregulate some neural genes and downregulate pluripotency genes, this suggests that FGF-MEK signaling may be directly repressing neural genes in hESCs, as has been shown in mEpiSCs [51]. The combination of SMAD7 induction and early MEK inhibition strongly promotes expression of neural genes, coupled with downregulation of pluripotency genes, and results in robust neural conversion of hESCs.

Combined SMAD7 Induction and MEK Inhibition Promotes Anterior Neural Fate

MEK inhibition was then tested to ascertain whether it alters the anterior neural profile imposed by SMAD7 induction alone. In addition to promoting neural fate, qPCR confirmed that combined MEK and TGFβ inhibition also enhanced acquisition of an anterior fate. The MEK-I/SMAD7 combination enhanced expression of the forebrain transcription factor FOXG1, as compared to SMAD7 induction alone (Fig. 5E) and resulted in ~10-fold greater expression of FOXG1 transcripts at Day 7, the last time point tested. This was also confirmed by IF (data not shown). Like SMAD7 alone, these changes were also direct and did not significantly induce non-neural lineage genes, as evidenced by absence of expression of mesoderm, endoderm, non-neural ectoderm, and trophectoderm lineage markers (supporting information Fig. S5A, S5B). Importantly, the neural crest marker SOX10 was also not induced in the MEK-I/SMAD7 combination (supporting information Fig. S5A). Interestingly, MEK-I alone could also upregulate FOXG1 to a greater extent than the SMAD7-only condition, although to a considerably lesser extent than that of the MEK-I/SMAD7 combination, suggesting that MEK1/2-ERK and TGFβ-SMAD signaling might be regulating FOXG1 expression during development. In addition, higher expression levels were seen for the forebrain determinant LHX2 at Day 7 (three-folds) as well as the rostral neural gene ZNF521 (25-fold) between Days 5 and 7 in the MEK-I/SMAD7 combination compared to SMAD7-only conditions. Comparable expression of OTX2 was observed until Day 3, after which lower levels were observed (Fig. 5E). Based on these results, we conclude that combined inhibition of FGF-MEK and TGFβ-SMAD signaling significantly accelerates the acquisition of neural fate in hESCs without changing the anterior character of the cells.

Discussion

These results demonstrate that the fundamental principles of neural conversion are conserved between pluripotent amphibian cap cells and hESCs. Cell-intrinsic inhibition of the two branches of TGFβ signaling via the inhibitory SMAD (SMAD7) is sufficient to impose a neural fate in hESCs without inducing non-neural lineages. This neuroepithelium is of anterior character as defined by several criteria. Significantly, this conversion can take place efficiently—even under pluripotency conditions. While inhibition of Activin/Nodal signaling alone has been shown to promote neural fate in hESCs, the neural fate has been shown to be of caudal character, presumably due to autocrine BMP signaling and/or concurrent induction of non-neural cell types, which in turn may act as secondary induction centers [16, 52]. A previous study demonstrated that inhibition of Activin/Nodal-SMAD2/3 and BMP-SMAD1/5/8 pathways with small molecule inhibitors of ALK receptors enables anterior neural conversion [14]. However, this protocol gives rise to heterogeneous neural differentiation, with concurrent induction of both neural crest and neural lineages. Cell density has a drastic effect on the outcome in this system, with low densities failing to neuralize and higher densities promoting a CNS fate. This is likely due to incomplete inhibition of the TGFβ branches by the small molecules at low cell densities that is compensated at higher densities by activation of the Hippo-TAZ/YAP pathway, which in turn can contribute to SMAD inhibition [53]. In the SMAD7-induction protocol, we did not generate neural crest derivatives and saw efficient neuralization at low densities. The uniform induction seen in our system may be a result of potent cell-intrinsic TGFβ inhibition by SMAD7, which occurs in both the cytoplasm and the nucleus. SMAD7 acts at many nodes to achieve this inhibition, including degradation of ALK receptors, disruption of receptor SMAD binding, inhibition of SMAD4-DNA complex formation in the nucleus, and recruitment of transcriptional repressors to SMAD binding sites [21]. Additionally, SMAD7 has also been shown to inhibit WNT signaling in some cellular contexts [54]. This activity may potentially be contributing to the efficient neural conversion observed here in the absence of neural crest lineages [55]. While we show loss of R-SMAD activity in SMAD7-induced hESCs, the possibility remains that SMAD7 may also be inhibiting noncanonical (i.e., non-R-SMAD mediated) branches of TGFβ signaling which in turn may also be contributing to neuralization. It is worth mentioning that the anterior character of the SMAD7-induced neuroepithelium demonstrated here is comparable to that seen with small molecule inhibitors of TGFβ signaling, suggesting that inhibition of Activin/Nodal and BMP signaling pathways in hESCs is the primary mechanism of action of SMAD7.

Pluripotency and self-renewal of hESCs are maintained by three highly interwoven signaling pathways: FGF, Activin/Nodal, and WNT (Fig. 6) [7, 32, 56]. While other studies have demonstrated an inhibitory role for Activin/Nodal and WNT signaling in neural induction in hESCs [40, 57, 58], the role of FGF-MEK has remained controversial. FGF maintains pluripotency in hESCs by transducing signal through sequential phosphorylation of MEK1/2 (MAPKK) and ERK1/2 (MAPK) [46]. In other vertebrates, FGF-MEK has been proposed to play an active role in neuralization by various mechanisms [59]. An essential role for FGF-MEK has also been proposed for neural induction in mouse ESCs [48] as well as hESCs [47]. More recent studies have challenged these results [50, 51], instead suggesting that FGF-MEK signaling promotes the transition of mESCs to mEpiSCs, which in turn gain competence to give rise to the different germ layers found in the embryo. Indeed, inhibition of MEK in mESCs blocks their transition into an

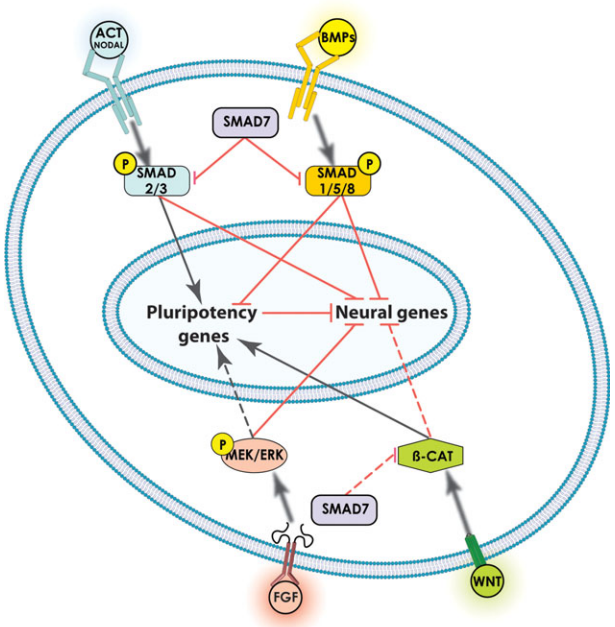

Figure 6. Proposed model showing that primed pluripotent state requires inhibition of the default neural state. Schematic showing that the three pathways mediating pluripotency in human embryonic stem cells: FGF-MEK, WNT-β- CATENIN, and ACTIVIN/NODAL-SMAD2/3 may repress neural fate directly and indirectly via pluripotency genes like NANOG. We propose that the state of pluripotency requires inhibition of the default state of differentiation, that is, the neural fate. Arrows represent activation while hatches represent inhibition. Dotted lines denote postulated mechanisms from evidence in mouse ESCs. Abbreviations: BMP, bone morphogenetic protein; FGF, fibroblast growth factor.

epiblast state [49]. Hence, in this model, FGF-MEK regulates the competence of mESCs for germ layer differentiation, rather than neural induction per se. It would be expected from this model that Activin/Nodal and BMP inhibition should be sufficient to impose an anterior neural fate on mEpiSCs; indeed this has been shown to be the case [60].

Our functional studies, guided by time course gene expression analysis during SMAD7 neural induction, reveal that FGF-MEK has an inhibitory, rather than an instructive role in neural induction in hESCs in the presence of inhibitory TGFβ signals. Conversely, this implies that repression of a neural fate by FGF-MEK is essential for its role in maintaining pluripotency in hESCs. This may be accomplished in part by promoting NANOG expression [30, 46] and/or by directly repressing neural genes (Fig. 6) [30, 51]. Likewise, Activin/Nodal-SMAD2/3 signaling also promotes NANOG expression and represses a neural fate in hESCs [29, 40]. In concert with these pathways, WNT signaling also contributes to pluripotency in hESCs [56], and inhibition of WNT signaling also promotes neural induction in hESCs through mechanisms that remain unknown [57, 58]. These observations point to a model where maintenance of the primed state of pluripotency requires inhibition of the default state of differentiation of hESCs, namely, the neural fate (Fig. 6). In this context, inhibition of the BMP-SMAD1/5/8 branch may serve to (a) promote expression of cell-intrinsic anterior neural inducers such as ZNF521 [38], (b) inhibit non-neural ectodermal and trophectodermal differentiation resulting from autocrine BMP ligands [7, 62], and (c) stabilize the neural differentiation program for instance, by maintaining expression of SOX2 [61,62]. Combined inhibition of Activin/Nodal and BMP branches of signaling has been shown to be required for optimal neural induction in vivo during *Xenopus* development [63]. Similar to what we show here in hESCs, FGF-MEK has also been shown to repress neuroectodermal differentiation in mEpiSCs [51]. These results are in contrast to what has been suggested previously by other groups [47]; this discrepancy is likely explained by the requirement of FGF-MEK signaling for secretion of BMP inhibitors in the system used in that study [4]. In the presence of *a priori* SMAD1/5/8 inhibition (for instance by SMAD7 in our case), FGF-MEK signaling is not instructive to a neural fate.

Mouse ESCs are thought to exist in a naïve or "ground" state of pluripotency, which represents an immature state that permits maintenance of pluripotency and self-renewal in the absence of extrinsic stimuli using a cocktail of inhibitors of FGF receptor, MEK, and GSK3β [39, 64]. In contrast, mEpiSCs represent a later more mature stage of development and are more amenable or primed for differentiation [39]. hESCs share multiple defining features with mEpiSCs including signaling characteristics, morphology, and X-chromosomal inactivation and are thought to closely resemble the primed pluripotent state of mEpiSCs rather than the naïve state of mESCs [39]. Our study extends these findings and suggests that maintenance of the primed pluripotent state of hESCs, and perhaps mEpiSCs, may require inhibition of the default state, that is, neural differentiation, which is achieved by activation of FGF-MEK, TGFβ-SMAD, and WNT pathways. Further studies are needed to conclusively verify this model.

Lastly, the protocol described here will be useful for efficient generation of anterior neural precursors under chemically defined conditions. While SMAD7 induction alone could generate a population of neural cells by Day 12 of induction, addition of a MEK-inhibitor accelerated this process to Day 7. With recent advances in directly introducing mRNAs into hESCs, this protocol could potentially be adapted for a wide range of hESC and human induced pluripotent stem cells (hiPSC) lines for transgene-free neural conversion. We anticipate that refractory hiPSCs will also be more responsive to SMAD7 induction, since unlike small-molecule-based protocols SMAD7 acts cell-intrinsically to inhibit the receptor SMADs. The system described here provides a useful tool for genetically inducible neural conversion of hESCs and suggests that the default model may have implications for disease modeling and clinical applications.

While our results suggest that inhibition of FGF-MEK promotes neural induction in our system, we cannot at this time rule out the possibility that other branches of FGF signaling may have a role in neural induction. It is worth noting that that inhibition of the FGF receptor together with SMAD7 induction does result in accelerated neural conversion in our system, as has been reported previously in other protocols of neural conversion [51]. However, it is plausible that different branches of FGF signaling may have opposite roles in neural induction, and this will need to be addressed in future studies. Our genetically inducible system of neural induction provides a platform for such studies and will permit detailed interrogation of the earliest stages of neural specification and fate choices.

Conclusions

These results together show that SMAD7—a cell-intrinsic inhibitor of Activin/Nodal and BMP signaling—is sufficient to confer an anterior neural fate on pluripotent hESCs. Time course gene expression analysis of SMAD7-mediated neural induction demonstrates downregulation of MAPK signaling components. In agreement with this, combining MEK1/2 inhibition with SMAD7-mediated TGFβ inhibition promoted telencephalic

conversion. FGF-MEK and TGFβ-SMAD signaling maintain hESCs by promoting pluripotency genes and repressing neural genes. Our findings suggest that in the absence of these cues, pluripotent cells simply revert to a program of neural conversion. Hence, the primed state of hESCs requires inhibition of the default state of neural fate acquisition. This has parallels in amphibians, suggesting an evolutionarily conserved mechanism.

Acknowledgments

We would like to acknowledge the contributions of Marie Knockaert for the Western blot data and Blaine Cooper for his generous assistance in making the Figures. We would also like to thank members of the Brivanlou Lab for useful discussions on the manuscript. This work was supported by the following research grants: a New York State Stem Cell Initiative (NYSTEM) Shared Facilities Grant, NIH Grant 2R01HD032105, and private funding from The Rockefeller University. S.N. is currently affiliated with the The New York Stem Cell Foundation, 1995 Broadway, NY.

Disclosure of Potential Conflicts of Interest

The authors indicate no potential conflicts of interest.

References

1 Spemann H, Mangold H. Induction of embryonic primordia by implantation of organizers from a different species. 1923. Int J Dev Biol 2001;45:13–38.
2 Hemmati-Brivanlou A, Melton DA. A truncated activin receptor inhibits mesoderm induction and formation of axial structures in Xenopus embryos. Nature 1992;359:609–614.
3 Hemmati-Brivanlou A, Melton DA. Inhibition of activin receptor signaling promotes neuralization in Xenopus. Cell 1994;77:273–281.
4 Munoz-Sanjuan I, Brivanlou AH. Neural induction, the default model and embryonic stem cells. Nat Rev Neurosci 2002;3:271–280.
5 Poorgholi Belverdi M, Krause C, Guzman A et al. Comprehensive analysis of TGF-beta and BMP receptor interactomes. Eur J Cell Biol 2012;91:287–293.
6 Taylor IW, Wrana JL. SnapShot: The TGFbeta pathway interactome. Cell 2008;133:378 e1.
7 Xu RH, Peck RM, Li DS et al. Basic FGF and suppression of BMP signaling sustain undifferentiated proliferation of human ES cells. Nat Methods 2005;2:185–190.
8 Yu P, Pan G, Yu J et al. FGF2 sustains NANOG and switches the outcome of BMP4-induced human embryonic stem cell differentiation. Cell Stem Cell 2011;8:326–334.
9 Liu A, Niswander LA. Bone morphogenetic protein signalling and vertebrate nervous system development. Nat Rev Neurosci 2005;6:945–954.
10 Levine AJ, Brivanlou AH. Proposal of a model of mammalian neural induction. Dev Biol 2007;308:247–256.
11 Stern CD. Neural induction: 10 years on since the 'default model'. Curr Opin Cell Biol 2006;18:692–697.
12 Camus A, Perea-Gomez A, Moreau A et al. Absence of Nodal signaling promotes precocious neural differentiation in the mouse embryo. Dev Biol 2006;295:743–755.
13 Bachiller D, Klingensmith J, Kemp C et al. The organizer factors Chordin and Noggin are required for mouse forebrain development. Nature 2000;403:658–661.
14 Chambers SM, Fasano CA, Papapetrou EP et al. Highly efficient neural conversion of human ES and iPS cells by dual inhibition of SMAD signaling. Nat Biotechnol 2009;27:275–280.
15 Li W, Sun W, Zhang Y et al. Rapid induction and long-term self-renewal of primitive neural precursors from human embryonic stem cells by small molecule inhibitors. Proc Natl Acad Sci USA 2011;108:8299–8304.
16 Smith JR, Vallier L, Lupo G et al. Inhibition of Activin/Nodal signaling promotes specification of human embryonic stem cells into neuroectoderm. Dev Biol 2008;313:107–117.
17 Watanabe K, Kamiya D, Nishiyama A et al. Directed differentiation of telencephalic precursors from embryonic stem cells. Nat Neurosci 2005;8:288–296.
18 Pankratz MT, Li XJ, Lavaute TM et al. Directed neural differentiation of human embryonic stem cells via an obligated primitive anterior stage. Stem Cells 2007;25:1511–1520.
19 Ying QL, Stavridis M, Griffiths D et al. Conversion of embryonic stem cells into neuroectodermal precursors in adherent monoculture. Nat Biotechnol 2003;21:183–186.
20 Casellas R, Brivanlou AH. Xenopus Smad7 inhibits both the activin and BMP pathways and acts as a neural inducer. Dev Biol 1998;198:1–12.
21 Yan X, Z Liu, Y Chen. Regulation of TGF-beta signaling by Smad7. Acta Biochim Biophys Sin 2009;41:263–272.
22 Pogoda HM, Meyer D. Zebrafish Smad7 is regulated by Smad3 and BMP signals. Dev Dyn 2002;224:334–349.
23 Zwijsen A, van Rooijen MA, Goumans MJ et al. Expression of the inhibitory Smad7 in early mouse development and upregulation during embryonic vasculogenesis. Dev Dyn 2000;218:663–670.
24 Zhang L, Huang H, Zhou F et al. RNF12 controls embryonic stem cell fate and morphogenesis in zebrafish embryos by targeting Smad7 for degradation. Mol Cell 2012;46:650–661.
25 Chen Q, Chen H, Zheng D et al. Smad7 is required for the development and function of the heart. J Biol Chem 2009;284:292–300.
26 Li R, Rosendahl A, Brodin G et al. Deletion of exon I of SMAD7 in mice results in altered B cell responses. J Immunol 2006;176:6777–6784.
27 Tojo M, Takebe A, Takahashi S et al. Smad7-deficient mice show growth retardation with reduced viability. J Biochem 2012;151:621–631.
28 Weng Q, Chen Y, Wang H et al. Dual-mode modulation of Smad signaling by Smad-interacting protein Sip1 is required for myelination in the central nervous system. Neuron 2012;73:713–728.
29 Chng Z, Teo A, Pedersen RA et al. SIP1 mediates cell-fate decisions between neuroectoderm and mesendoderm in human pluripotent stem cells. Cell Stem Cell 2010;6:59–70.
30 Greber B, Coulon P, Zhang M et al. FGF signalling inhibits neural induction in human embryonic stem cells. EMBO J 2011;30:4874–4884.
31 Vallier L, Alexander M, Pedersen RA. Activin/Nodal and FGF pathways cooperate to maintain pluripotency of human embryonic stem cells. J Cell Sci 2005;118:4495–4509.
32 James D, Levine AJ, Besser D et al. TGFbeta/activin/nodal signaling is necessary for the maintenance of pluripotency in human embryonic stem cells. Development 2005;132:1273–1282.
33 Rosa A, Spagnoli FM, Brivanlou AH. The miR-430/427/302 family controls mesendodermal fate specification via species-specific target selection. Dev Cell 2009;16:517–527.
34 Watanabe K, Ueno M, Kamiya D et al. A ROCK inhibitor permits survival of dissociated human embryonic stem cells. Nat Biotechnol 2007;25:681–686.
35 Lacoste A, Berenshteyn F, Brivanlou AH. An efficient and reversible transposable system for gene delivery and lineage-specific differentiation in human embryonic stem cells. Cell Stem Cell 2009;5:332–342.
36 James D, Noggle SA, Swigut T et al. Contribution of human embryonic stem cells to mouse blastocysts. Dev Biol 2006;295:90–102.
37 Suarez-Farinas M, Noggle S, Heke M et al. Comparing independent microarray studies: The case of human embryonic stem cells. BMC Genomics 2005;6:99.
38 Kamiya D, Banno S, Sasai N et al. Intrinsic transition of embryonic stem-cell differentiation into neural progenitors. Nature 2011;470:503–509.
39 Hanna JH, Saha K, Jaenisch R. Pluripotency and cellular reprogramming: Facts, hypotheses, unresolved issues. Cell 2010;143:508–525.
40 Vallier L, Mendjan S, Brown S et al. Activin/Nodal signalling maintains pluripotency by controlling Nanog expression. Development 2009;136:1339–1349.
41 Boyer LA, Lee TI, Cole MF et al. Core transcriptional regulatory circuitry in human embryonic stem cells. Cell 2005;122:947–956.
42 Rosa A, Brivanlou AH. A regulatory circuitry comprised of miR-302 and the transcription factors OCT4 and NR2F2 regulates human embryonic stem cell differentiation. EMBO J 2011;30:237–248.
43 Wang Z, Oron E, Nelson B et al. Distinct lineage specification roles for NANOG, OCT4, and SOX2 in human embryonic stem cells. Cell Stem Cell 2012;10:440–454.
44 Tamplin OJ, Kinzel D, Cox BJ et al. Microarray analysis of Foxa2 mutant mouse embryos reveals novel gene expression and inductive roles for the gastrula organizer and its derivatives. BMC Genomics 2008;9:511.
45 Goulding MD, Chalepakis G, Deutsch U et al. Pax-3, a novel murine DNA binding protein expressed during early neurogenesis. EMBO J 1991;10:1135–1147.

46 Chen G, Gulbranson DR, Yu P et al. Thermal stability of FGF protein is a determinant factor in regulating self-renewal, differentiation and reprogramming in human pluripotent stem cells. Stem Cells 2012;30: 623–630.
47 LaVaute TM, Yoo YD, Pankratz MT et al. Regulation of neural specification from human embryonic stem cells by BMP and FGF. Stem Cells 2009;27:1741–1749.
48 Stavridis MP, Lunn JS, Collins BJ et al. A discrete period of FGF-induced Erk1/2 signalling is required for vertebrate neural specification. Development 2007;134:2889–2894.
49 Kunath T, Saba-El-Leil MK, Almousailleakh M et al. FGF stimulation of the Erk1/2 signalling cascade triggers transition of pluripotent embryonic stem cells from self-renewal to lineage commitment. Development 2007;134:2895–2902.
50 Sterneckert J, Stehling M, Bernemann C et al. Neural induction intermediates exhibit distinct roles of Fgf signaling. Stem Cells 2010;28: 1772–1781.
51 Greber B, Wu G, Bernemann C et al. Conserved and divergent roles of FGF signaling in mouse epiblast stem cells and human embryonic stem cells. Cell Stem Cell 2010;6:215–226.
52 Patani R, Compston A, Puddifoot CA et al. Activin/Nodal inhibition alone accelerates highly efficient neural conversion from human embryonic stem cells and imposes a caudal positional identity. PLoS One 2009;4:e7327.
53 Varelas X, Samavarchi-Tehrani P, Narimatsu M et al. The Crumbs complex couples cell density sensing to Hippo-dependent control of the TGF-beta-SMAD pathway. Dev Cell 2010;19:831–844.
54 Han G, Li AG, Liang YY et al. Smad7-induced beta-catenin degradation alters epidermal appendage development. Dev Cell 2006;11: 301–312.
55 Menendez L, Yatskievych TA, Antin PB et al. Wnt signaling and a Smad pathway blockade direct the differentiation of human pluripotent stem cells to multipotent neural crest cells. Proc Natl Acad Sci USA 2011;108:19240–19245.
56 Sato N, Meijer L, Skaltsounis L et al. Maintenance of pluripotency in human and mouse embryonic stem cells through activation of Wnt signaling by a pharmacological GSK-3-specific inhibitor. Nat Med 2004;10:55–63.
57 Eiraku M, Watanabe K, Matsuo-Takasaki M et al. Self-organized formation of polarized cortical tissues from ESCs and its active manipulation by extrinsic signals. Cell Stem Cell 2008;3:519–532.
58 Fasano CA, Chambers SM, Lee G et al. Efficient derivation of functional floor plate tissue from human embryonic stem cells. Cell Stem Cell 2010;6:336–347.
59 Stern CD. Neural induction: Old problem, new findings, yet more questions. Development 2005;132:2007–2021.
60 Najm FJ, Zaremba A, Caprariello AV et al. Rapid and robust generation of functional oligodendrocyte progenitor cells from epiblast stem cells. Nat Methods 2011;8:957–962.
61 Greber B, Lehrach H, Adjaye J. Control of early fate decisions in human ES cells by distinct states of TGFbeta pathway activity. Stem Cells Dev 2008;17:1065–1077.
62 Kim H, Lee G, Ganat Y et al. miR-371-3 expression predicts neural differentiation propensity in human pluripotent stem cells. Cell Stem Cell 2011;8:695–706.
63 Chang C, Harland RM. Neural induction requires continued suppression of both Smad1 and Smad2 signals during gastrulation. Development 2007;134:3861–3872.
64 Ying QL, Wray J, Nichols J et al. The ground state of embryonic stem cell self-renewal. Nature 2008;453:519–523.

See www.StemCells.com for supporting information available online.